Structural Analysis of Historical Constructions, New Delhi 2006
P.B. Lourenço, P. Roca, C. Modena, S. Agrawal (Eds.)

A Specific Rigid Element Model for Macro-Scale Dynamics of Monumental Masonry considering Damage and Micro-Structure Effects

Siro Casolo
Politecnico di Milano, Dipartimento di Ingegneria Strutturale, Italy

ABSTRACT: The paper presents a specific computational model for the in-plane dynamical analysis of masonry walls subjected to earthquakes. The model formulation is based on two main considerations: i) the building performance is related to the energy dissipation capacity of the material; ii) the damage mechanisms are influenced by the masonry texture. Clearly, non-linear dynamics requires models with few degrees of freedom together with the assumption of simplified hypotheses about the material response. As a consequence, it is essential to balance the needs of an adequate description of the building geometry with a realistic post-elastic material modelling. To do this, the proposed method adopts rigid elements connected by line springs that are defined in order to obtain a phenomenological description of the cyclic response and degradation of the masonry material. The proposed mechanistic formulation is presented in the frame of a global seismic analysis of a real masonry monument.

1 INTRODUCTION

The seismic analysis of monumental masonry buildings is the main interest of the present research. These structures have specific architectonic parts, such as large façades, pillars, slender columns, arches and vaults that often suffer damage and mechanical degradation even when subjected to moderate earthquakes. In this case, in order to obtain a reliable estimation of the seismic risk, it is desirable to perform full dynamical analyses that describe the effective transmission and dissipation of the energy coming from the ground motion into the structure (Bertero, 2002; Housner, 1970; Petrini and Casolo, 2002; Uang and Bertero, 1990).

At present, modelling the non-linear mechanical behaviour of masonry monuments by means of three-dimensional models require a great amount of computational resources that are not commonly available. Luckily, it is often effective to subdivide these monuments into "macro-elements" (e.g. the façade, the lateral walls, the triumphal arch, the bell tower, the apse), since the seismic response of these single parts tends to be dominated by recurrent damage mechanisms, and the mechanical interrelation between contiguous parts is limited (Doglioni et al., 1994; Petrini et al., 1999). In particular, when performing complete dynamical analyses it is often preferable to adopt a two-dimensional model rather than a three-dimensional (Lourenço, 2002), even if the definition of a simpler model often requires a process of tuning in order to approximate as well as possible the features of the specific kinematics that is of interest.

In the present paper this strategy is applied to the seismic analysis of the large medieval

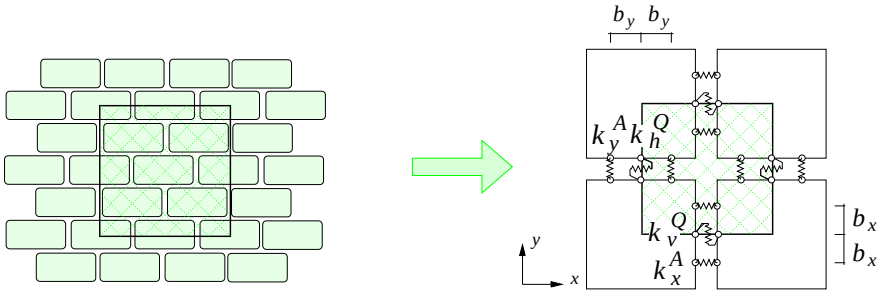

Figure 1: Scheme of a regular masonry texture and an example of "unit cell" made of rigid elements connected by line springs.

"Maniace Castle", in Siracusa, Italy, by using three different numerical models: i) a global three-dimensional finite element model of the whole castle; ii) a detailed three-dimensional finite element model of the architectural part of the building that suffered the main static problems; iii) a two-dimensional rigid element model by which the dynamical analysis are done by considering the degradation of the material subjected to cyclic loading.

The first two models have been only used for doing linear-elastic analyses, while the third model is actually the specific contribute of this paper. The proposed model has been formulated with the aim to investigate the seismic damage to the pillars, the buttresses and the arches of the masonry monuments, and in particular it is designed to work at a "meso-scale" that lies between the "micro-scale" at which the masonry is described in terms of single material components (blocks and mortar joints), and the "macro-scale" at which the masonry can be globally described by a Cauchy homogeneous continuum. As shown in the scheme of Figure 1, the quadrilateral rigid elements are connected at each side by three elastic-plastic devices that can be imaged as simple line springs (Casolo, 2004). The elastic characteristics of these springs are defined by a specific procedure of identification with the objective to transfer some "memory" of the texture's characteristics to the discrete meso-scale model (Casolo, 2006). This could be of particular interest when the degradation of the mortar joints under heavy loading cause an evolution of the micro-structure characteristics. The material response under cyclic loading is modelled by means of a simplified phenomenological approach (Boffi and Casolo, 1998; Casolo and Peña, 2004), based on the experimental tests available in the technical literature.

2 THREE MODELS FOR THE CASTLE

2.1 The global three-dimensional finite element model

As first, the global behaviour of "Maniace Castle" has been studied by means of a large three-dimensional finite element model with a total number of 108625 solid tetrahedron elements, named *C3D4* in the adopted *Abaqus* computer code (Hibbitt et al., 2005). In this model the geometric details have been simplified by disregarding the exact three-dimensional shape of the internal vaults, as well as many other structural details. On the other hand, the elastic characteristics given to the different construction materials are assigned in substantial accord with the data already published about this building (Modena et al., 2001). After a brief process of tuning, this model was capable to approximate the basic fundamental modes of vibration as well as the mean values of stress due to the gravity in the most critical parts of the building, the columns and the buttresses, as

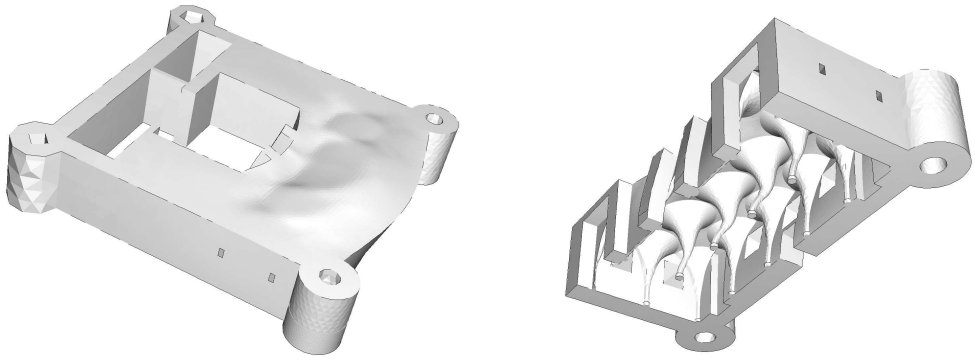

Figure 2: Deformed shape of the first natural mode of vibration of the whole castle.

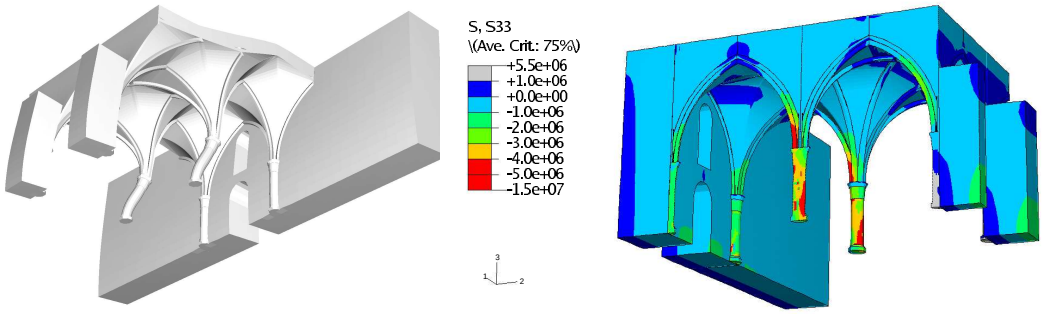

Figure 3: Deformed shape of the first natural mode of vibration of the detailed model of the hypostyle chamber (left) and distribution of the vertical axial stress S_{33} [Pa] caused by the action of gravity plus a lateral acceleration equal to 2.5 m/s^2 (right).

it resulted from the previously published experimental and computational studies. Two images of the deformed shape corresponding to the first natural mode of vibration, with a frequency of 5.6 Hz, are shown in Figure 2.

2.2 The partial three-dimensional finite element model

The numerical analysis made on the whole Castle has shown that in the case of seismic excitation the most critical part of the building is the vaulted room, i.e. the rest of the ancient hypostyle chamber named "Salone". In particular, it is at risk the load bearing capacity of the four columns and of the two buttresses in the internal courtyard. Thus, a refined three-dimensional finite element model has been assembled in order to get a deeper knowledge of the kinematics and the stress situation of this part of the building in the linear elastic field. In this case, the geometry is modelled with great detailed, and the real shape of the cross-vaults, the ribs, and all the structural details that can be significant for the stress analysis have been implemented. Moreover, the different construction materials adopted in the real building could be assigned with some precision within the limits of the linear elastic field. This detailed model has a total number of 48004 8-node brick elements, named *C3D8* in the adopted *Abaqus* computer code (Hibbitt et al., 2005). Figure 3 shows the deformed shape that corresponds to the first natural mode of vibration of this partial model, with a frequency of 4.6 Hz, while the map of the vertical axial stress is shown for the case in which the model was loaded by the vertical acceleration of gravity plus a lateral acceleration equal to 2.5 m/s^2. Such value of acceleration is coherent with the seismic hazard of the site of the castle, in Siracusa.

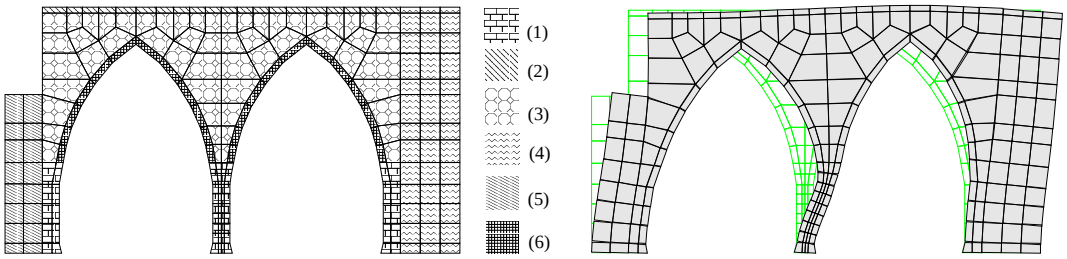

Figure 4: Left: rigid element model with indication of the 6 different materials assigned to the elements. Right: deformed shape corresponding to the first natural mode of vibration, at 4.8 Hz.

2.3 The two-dimensional rigid element model

Since the geometry of the proposed two-dimensional model is very simple, in this case it was necessary to perform a fine tuning on the characteristics the different materials that constitute the model in order to approximate the real three-dimensional behaviour. Six different materials have been assigned to this discrete model, as shown in Figure 4, on the left. Some of the characteristics of these materials are reported in Table 2, together with the thickness given to the corresponding elements. The numerical response of this model proved to be satisfactory in the linear elastic field. The first natural mode of vibration is in good agreement with the previous finite element models, both in terms of frequency and of global shape, shown in Figure 4. Moreover, also the estimated values of stress are correct, in particular for what regards the vertical axial component in the columns and in the buttress that are the more critical parts of this structure.

Table 1: Characteristics given to the different materials and elements' thickness.

Material	Density (Kg/m^3)	E_x/E_y (MPa)	$2G$ (MPa)	Thickness (m)
(1) Columns	2200	8000 / 10000	7500	0.75
(2) Roof	1000	1000	833	8.7
(3) Infill of the vault	1000	700	650	3.5
(4) Perimeters main wall	1800	4000 / 5000	3500	8.7
(5) Buttress	1800	4000 / 5000	3500	1.2
(6) Arches and vault	2200	5000	4000	4.75

3 SHORT SUMMARY OF THE RIGID ELEMENT APPROACH

3.1 Kinematics and balance equations

The model geometry and the kinematics are described by considering the mid-plane of the structure $\Omega \subset \Re^2$ in a global Cartesian coordinate frame $\{O, x, y\}$. The domain Ω is then partitioned into m quadrilateral cells such that no vertex of one quadrilateral lies on the edge of another quadrilateral. As shown in Figure 5, left, a local reference frame $\{o^i, \xi^i, \eta^i\}$ is fixed in the element barycentre o^i, with the ξ^i-axis initially parallel to the global x-axis. For each element ω^i, the three kinematic variables are the two translations u_i, v_i and the rotation angle ψ_i, and the whole deformed configuration is described by the $3m$ Lagrangian coordinates assembled into vector $\{u\}$,

$$\{u\}^T = \{u_1, v_1, \psi_1, u_2, v_2, \psi_2, \ldots, u_m, v_m, \psi_m\} \tag{1}$$

while the external loads, including the inertial forces, are assembled into a vector of

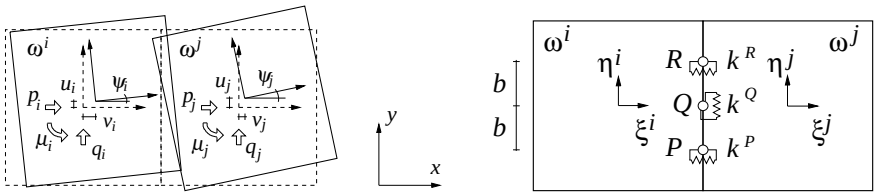

Figure 5: A couple of rigid elements with the adopted notation.

generalized external loads $\{p\}$, work-conjugated with $\{u\}$, as follows:

$$\{p\}^T = \{p_1, q_1, \mu_1, p_2, q_2, \mu_2, \ldots, p_m, q_m, \mu_m\} \tag{2}$$

Three connection points named P, Q and R are defined for each side in common between two adjoining rigid elements, as shown in Figure 5, right. In these points, the connecting devices can be thought as linear springs whose elastic force depend on the measure of mean strain associated to the corresponding point. In particular, a mean measure of shear strain ε^Q is associated with point Q, while two axial strains, ε^P and ε^R, are associated to points P and R. These measures are assembled in vector $\{\varepsilon\}$, and assuming small displacements, the linearity allows to express the strain-displacement relations by considering a $3r \times 3m$ matrix $[B]$ as follows:

$$\{\varepsilon\} = [B]\{u\} \tag{3}$$

being r the number of sides that connect the elements of the whole discrete model (Casolo, 2004). A vector of generalized stresses $\{\sigma\}$ is correspondingly assembled, together with the diagonal matrices $[V]$ and $[D]$ that contain the volumes of pertinence and the elastic stiffnesses of all the springs:

$$\{\sigma\}^T = \left\{\sigma_1^P, \sigma_1^Q, \sigma_1^R, \sigma_2^P, \sigma_2^Q, \sigma_2^R, \ldots, \sigma_r^P, \sigma_r^Q, \sigma_r^R\right\} \tag{4}$$

$$[V] = \mathrm{Diag}\left\{V_1^P, V_1^Q, V_1^R, V_2^P, V_2^Q, V_2^R, \ldots, V_r^P, V_r^Q, V_r^R\right\} \tag{5}$$

$$[D] = \mathrm{Diag}\left\{k_1^P, k_1^Q, k_1^R, k_2^P, k_2^Q, k_2^R, \ldots, k_r^P, k_r^Q, k_r^R\right\} \tag{6}$$

Given the constitutive relation for the connecting devices $\{\sigma\} = [D]\{\varepsilon\}$, the principle of virtual work is written as follows:

$$\{\overline{u}\}^T\{p\} = \overline{W}_E = \overline{W}_I = \{\overline{\varepsilon}\}^T[V]\{\sigma\} = \{\overline{u}\}^T[B]^T[V][D][B]\{u\} \tag{7}$$

being $\overline{W}_E$ and $\overline{W}_I$ the external and internal virtual work. Thus, for each arbitrary virtual displacement $\{\overline{u}\}$ the following balance equation must hold:

$$\{p\} = [B]^T[V][D][B]\{u\} = [K]\{u\} \tag{8}$$

being $[K]$ the generalized stiffness matrix of the discrete system.

In order to consider the inertial forces, the mass of each element m_i and the rotational inertia about the barycentre ι_i, are assembled in the following diagonal matrix:

$$[M] = \mathrm{Diag}\,\{m_1, m_1, \iota_1, m_2, m_2, \iota_2, \ldots, m_m, m_m, \iota_m, \} \tag{9}$$

A viscous damping that acts essentially on the first few modes at low frequency is adopted by defining the viscous damping matrix $[C]$ as proportional to the mass matrix $[C] = a_0[M]$. Finally, in the general case of non-linear constitutive relation, the linearized

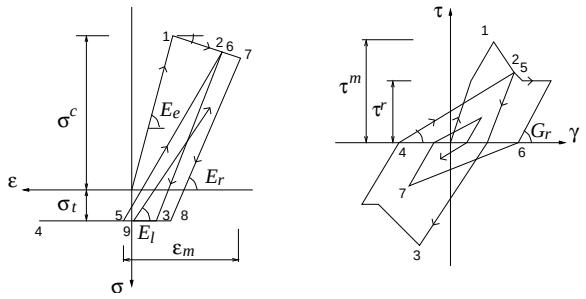

Figure 6: Hysteretic behaviour for the axial (left) and shear (right) connecting springs.

incremental form of the system of equations of the motion of the discrete system during a time interval can be expressed as follows:

$$[M]\{\ddot{u}\} + [C]\{\dot{u}\} + \{f^*\} + [K^*]\{\Delta u\} = \{p\} \tag{10}$$

being $\{f^*\}$ the vector of the internal generalized forces, and $[K^*]$ the generalized tangential stiffness matrix. The implicit method of Newmark is adopted to integrate this system of equations, performing full Newton-Raphson iterations until convergence is attained.

3.2 Material assumptions

The stiffnesses of the line springs, as well as the distance $2b$ between the axial connecting points are assigned with the criterion of approximating the strain energy in the corresponding volume of pertinence. A specific feature of present discrete model is the capability of transferring memory of the micro-scale original masonry texture also when adopting a coarse mesh, as explained in two papers recently published by Casolo (2004, 2006). In fact, some texture effects can be modelled by giving different stiffness to the vertical and horizontal shear springs and by giving an opportune distance $2b$ to the axial springs'. As a consequence, the model can approximate the interlocking of the original masonry blocks that can become significant when mortar joints are degraded. For the present application the hysteretic constitutive laws are assigned by adopting a phenomenological approach (Boffi and Casolo, 1998). These laws are macroscopic, based on experimental cyclic tests currently available in literature, e.g. Calvi and Magenes (1994), and should be assigned to rigid elements whose size is approximately comparable to the test specimens in order to limit the size effect problem. The laws proposed for the axial and the shear springs are shown in Figure 6. The strength of the horizontal shear springs is related to the vertical axial loading by a Coulomb-type relationship, assuming a coefficient of internal friction equal to 0.2.

Table 2: Some strength characteristics assigned to the six materials.

Material	σ_x^c / σ_y^c (MPa)	σ_x^t / σ_y^t (MPa)	τ_v^m / τ_h^m (MPa)	τ_v^r / τ_h^r (MPa)
(1) Columns	4.0 / 5.0	0.4 / 0.5	0.5 / 0.4	0.05/ 0.04
(2) Roof	1.0	0.1	0.1	0.01
(3) Infill of the vault	0.7	0.07	0.07	0.007
(4) External main wall	2.0 / 2.5	0.20 / 0.25	0.15 / 0.10	0.02 / 0.015
(5) Buttress	2.0 / 2.5	0.20 / 0.25	0.15 / 0.10	0.02 / 0.015
(6) Arches and vault	2.0 / 2.5	0.20 / 0.25	0.15 / 0.10	0.02 / 0.015

4 DYNAMICAL ANALYSIS

The main objective of the proposed discrete model is the execution of non-linear dynamical analyses with hysteretic and degrading characteristics assigned to the masonry

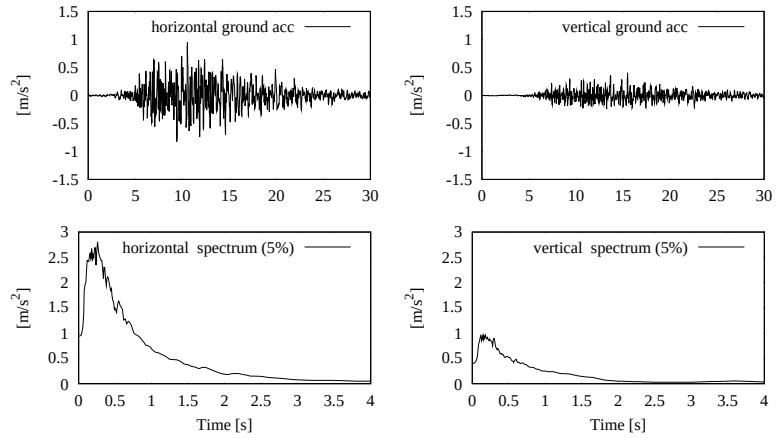

Figure 7: The accelerograms and their elastic response spectrum at 5% of damping.

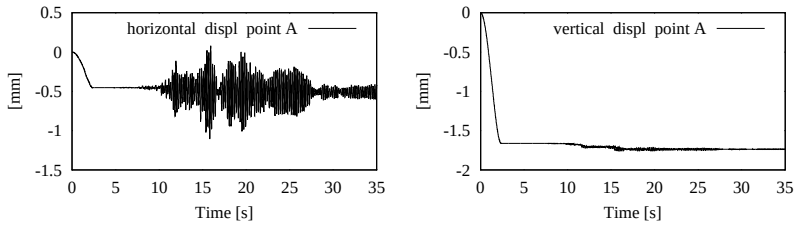

Figure 8: Time history of the displacement of point A (see Figure 9).

material. As an example, this paper presents the result of a seismic analysis in which the two-dimensional model is loaded by a couple of synthetic accelerograms, acting along the horizontal and the vertical direction. Figure 7 shows time history of the ground acceleration and the corresponding elastic response spectra, that are "compatible" with an estimated earthquake whose return period is 140 years for the site of this castle. The response in terms of time history of the displacements of a single point is shown in Figure 8 (this point is marked "A" in Figure 9). The analysis begins with the "ramp" application of the vertical gravity acceleration. Then, after five seconds, the dynamical analysis continues with the application of the ground motion while the gravity acceleration remains constant. At this point, the consequences of the seismic action can be investigated by comparing the deformed shape and the stress situation in the model, subjected to the simple vertical gravity acceleration, just *before* and *after* the application the seismic loading, as shown in the Figures 9 and 10. As expected, the critical elements are the buttress at the left side of the model, and the central column. The buttress mainly suffers damage due to the shear action that produces a marked permanent deformation together with a lose of lateral stiffness. The central column suffers the flexural deformation due to the lateral displacements that increase the static vertical axial compression reaching values that are close the strength of the material. Clearly, a realistic seismic risk estimation should employ more than a single dynamic analysis, this notwithstanding this example shows a possible way to enrich the investigations by means of a full dynamical model.

5 BIBLIOGRAPHY

Bertero V.V. 2002. Innovative approaches to earthquake engineering (Chapter 1). In G. Oliveto (ed.) *Innovative Approaches to Earthquake Engineering*, p. 1–54. WIT press.

Boffi G., Casolo S. 1998. Non-linear analyses of masonry arches. In *Workshop on seismic performance of monuments, Monument-98*, p. 99–108; Lisbon, November 12-14.

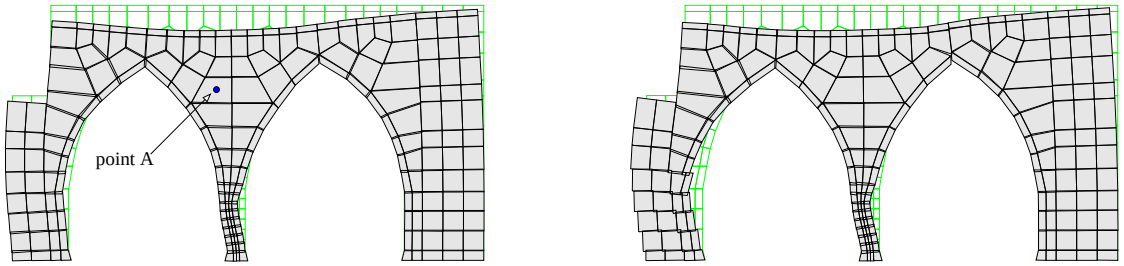

Figure 9: Deformed shape *before* (left) and *after* (right) the seismic loading.

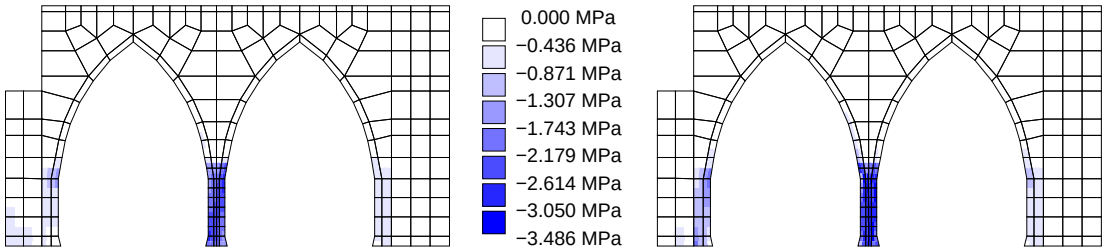

Figure 10: Vertical axial stress *before* (left) and *after* (right) the seismic loading.

Calvi G.M., G. Magenes. 1994. Experimental research on response of URM building systems. In *Proc. U.S.-Italian Workshop on guidelines for seismic evaluations and rehabilitations of unreinforced masonry buildings*, Pavia, June 22-24.

Casolo S. 2004. Modelling in-plane micro-structure of masonry walls by rigid elements. *International Journal of Solids and Structures* **41**(13), p. 3625–3641.

Casolo S., Peña F.. 2004. A specific rigid element approach for in-plane dynamic analyses of masonry structures. In *III Congreso Internacional sobre Métodos Numéricos en Ingeniería y Ciencias Aplicadas*, ITESM-CIMNE Monterrey, México, 22-24 Enero.

Casolo S. 2006. Macroscopic modelling of structured materials: relationship between orthotropic Cosserat continuum and rigid elements. *International Journal of Solids and Structures* **43**(3-4), p. 475–496.

Doglioni F., Moretti A., Petrini V. 1994. *Le Chiese e il Terremoto,* (in Italian). Lint press Trieste.

Hibbitt, Karlsson & Sorensen, Inc. (2005). ABAQUS Manuals. version 6.5.

Housner G.W. 1970. Strong ground motion. In Wiegel (ed.) *Earthquake Engineering*, p. 75–91. Prentice-Hall.

Lourenço P.B. 2002. Computations on historic masonry structures. *Progress in Structural Engineering and Materials* **4**(3), p. 301–319.

Modena C., Franchetti P., Zonta D., Menga R., Pizzigalli E., Ravasio F., Muti M., Meloni R., Bordone G. 2001. Static and dynamic analyses of "Maniace Castle" in Siracusa-Sicily. In P.B. Lourenço and P. Roca (eds.) *Historical Constructions,* p. 933–943. Guimaraes.

Petrini V., Casolo S., Doglioni F. 1999. Models for vulnerability analysis of monuments and strengthening criteria. In *Proceedings of the XI European Conference on Earthquake Engineering,* Paris; Invited lecture volume, p. 179–198. Baalkema.

Petrini V., Casolo S. 2002. Vulnerability of historical and monumental buildings: significant ground motion parameters and evaluation of the seismic performance (Chapter 4). In G. Oliveto (ed.) *Innovative Approaches to Earthquake Engineering,* p. 203–228. WIT press.

Uang C.-M., Bertero V.V. 1990. Evaluation of seismic energy in structures. *Earthquake Engineering and Structural Dynamics* **19**(1), p. 77–90.